

# The Formation of Rope- and Pebbles-Type Aggregation from the Micro-End-to-End and -Side-by-Side Aggregates in Poly(L-proline) Solutions

Hyun Don Kim

Samsung Chemicals Technology Center (Samsung Advanced Institute of Technology),

103-6, Moonji-Dong, Yusong-Gu, Taejeon 305-380, Korea

Received February 11, 1997

Morphological studies in the micro-end-to-end (m-E-E) and micro-side-by-side (m-S-S) aggregations were conducted by using of scanning electron microscope (SEM) for the samples precipitated by heating of the end-products of the transition of Form II (left-handed helix, three peptides per turn,  $3_1$ ) Form I (right-handed helix, 3.3 peptides per turn,  $10_3$ ) in poly(L-proline) (PLP) in acetic acid(water)-propanol (1:9 v/v) solvent. The observed morphology for the solid state shows a rope (or super helical) type and pebbles type aggregate for the (m-E-E) and (m-S-S) aggregate respectively. The viscosities were also measured during the heat-precipitation in order to elucidate the process of formation of the rope- and pebbles-type aggregates. The result for the (m-E-E) aggregations exhibit two steps, i.e., at first, the viscosity increases with time (step 1), thereafter it decrease until attain the last value (step 2). But the (m-S-S) aggregations show only one step in the decreases in viscosity. On the bases of all experimental results it is possible to propose a reasonable mechanism for the formation of the two types of aggregates of the (m-E-E) and (m-S-S).

## Introduction

In the conformational transition of Form II (left-handed helix, three peptides per turn,  $3_1$ ) to Form I (right-handed helix, 3.3 peptides per turn,  $10_3$ ) in poly(L-proline) (PLP), it was found in the previous report<sup>1,2</sup> that the intermolecular aggregation of Form I occurred accompanying the transition. Two types of aggregation were observed mainly, i.e., side-by-side (S-S) and end-to-end (E-E) types. The latter type aggregation is formed through the end group interaction between amino and carbonyl residues at each of the helical end, the former type is formed by mainly electrostatic (i.e., dipole-dipole) and van der Waals force (hydrophobic interaction) between the surfaces of the Form I helices.<sup>3</sup>

It was also noted that the aggregation type of the PLP Form I mainly depends on the solvents: the (S-S) type aggregation occurs favorably in aqueous medium, water-propanol (=W-PrOH) (1:9, etc. v/v), however the (E-E) type aggregation occurs in organic medium, acetic acid-propanol (=AcOH-PrOH) (1:9 v/v).

In the present study as a series of previous papers,<sup>1,2</sup> we try to observe a solid state morphologies of the Form I precipitates obtained by heating the micro-end-to-end (m-E-E) and micro-side-by-side (m-S-S) aggregation systems of the PLP by using SEM technique. [In here, the (m-E-E) and (m-S-S) aggregation means the (E-E) and (S-S) aggregations which existed in solution state.] In order to understand the observed morphology of the precipitates, the viscosities were also measured during the progress of precipitation. Finally from all the results in this study, we propose a reasonable mechanism for precipitation to explain the morphology of the precipitates.

## Experimental

### Materials

PLP (Form II) used in this study were purchased from Sigma Chem. Co. and the molecular weights  $M_n$  are 54,000, 31,000, 19,000 and 7,600. The propanol and acetic acid (Merk) were purified, and water was triply distilled. All the PLP samples are the same ones used in previous studies.<sup>1,2</sup>

### Measurements

**Scanning Electron Microscopy (SEM).** The morphology for the precipitates obtained from the micro Form I aggregates were observed by means of a scanning electron microscope (model ISI-SX-30E).

The preparation of samples for the microscopic observation are as follow: the aggregates of Form I obtained from Form II solution is heated in the solution at 65.5 °C in order to obtain precipitates. The precipitates are separated from the solvent, dried perfectly, and coated with a thin gold film.

**Viscometry.** Viscosities were measured in an automatic Ubbelohde-type viscometer. Temperature was controlled within  $\pm 0.02$  °C.

At temperature 65.5 °C, the outflow time for the AcOH-PrOH (1:9 v/v) solvent ( $t_0$ ) decreases slightly with time because of a small evaporation of one solvent in cosolvent system even though the degree of decrease is neglected. Thus the outflow time measured for the PLP solution was corrected by adding the degree of decrease in solvent time. The reduced viscosity ( $\eta_{red}$ ) is calculated by the equation,  $\eta_{sp}/C = [(t-t_0)/t_0]/C$ , where  $t$  is corrected outflow time for solution,  $\eta_{sp}$  exhibits the specific viscosity and  $C$  is the initial concentration of PLP. However, the outflow time W-PrOH (1:9 v/v) solvent is not varied nearly for a long time at 65.5 °C. Thus the correction is not necessary.

## Results and Discussion

Table 1 shows the  $\eta_{red}$  values for various PLP samples before the transition (Form II) and after a complete transition

**Table 1.** The  $\eta_{red}$  (dL/g) values at 25 °C before and after a complete transition-aggregation in the PLP with various  $M_v$  in two solvent systems [for all systems, the initial concentration of Form II before the transition Form II  $\rightarrow$  I  $C_0$  (Form II)=1.0 (ng/mL)]

$M_v$	AcOH-PrOH (1:9 v/v)		W-PrOH (1:9 v/v)	
	Form II' (before aggre.)	Form I (after aggre.)	Form II' (before aggre.)	Form I (after aggre.)
54,000	(a) 1.80	6.90 (E-E)	(c) 1.76	2.19 (S-S)
31,000	(b) 1.59	3.92 (E-E)	(d) 1.37	1.12 (S-S)
19,000			(e) 0.70	0.35 (S-S)
7,600			(f) 0.34	0.10 (no aggre.)

<sup>a</sup>Form II' is a state which exhibits specific optical rotation,  $-\alpha_D = 400$  (for the Form II,  $-\alpha_D = 540$ ). <sup>b</sup>Form I is a state which exhibits  $-\alpha_D = 15$ . <sup>c</sup>The (E-E) and (S-S) under the data indicate the aggregation types occurred in solutions.

accompanying possible aggregations (Form I) in the two solvents, AcOH-PrOH (1:9 v/v) and W-PrOH (1:9 v/v).

In the systems (a) and (b) in Table 1, one notes that  $\eta_{red}$  increased after a complete transition-aggregation. This is due to the (m-E-E) aggregation as mentioned in a previous report.<sup>1</sup> In the system (d) and (e) in Table 1, the decrease in  $\eta_{red}$  after the transition-aggregation is due to the (m-S-S) aggregation.<sup>2</sup> [Note: the aggregation types are shown under the data of  $\eta_{red}$  of the after aggregation column in Table 1.] One notes that in the (m-E-E) aggregation the chain length of PLP highly increases, inducing the increase in  $\eta_{red}$  in the systems. In the (m-S-S) aggregation, however, the PLP molecules become more compact making decrease in  $\eta_{red}$ . In the system (c), a small increase in viscosity after the transition-aggregation is caused by the existence of the (m-E-E) following the (m-S-S) aggregation about which mention was made already.<sup>2</sup>

### The Heat-Precipitation of PLP

Many authors<sup>4-8</sup> noted that when aqueous solution of PLP [Form II] was left at high temperature for a long time precipitation occurs and that the precipitation is promoted by increasing the temperature. One notes that in aqueous solution, the transition Form II  $\rightarrow$  Form I does not occur at all. The authors did not clarified the precipitates. We also observed that the solution of Form I of PLP which was ob-

tained from Form II solution by a complete transition-aggregation process makes precipitates when the solution was heated to 65.5 °C. In Table 2 are listed the time required for heating to make the precipitation. The heat-precipitation time ( $t_p$ ) is the time required for the Form I solution to develop a visual turbidity.

The  $t_p$  in Table 2 varies with types of aggregation of Form I at room temperature, i.e., in the (m-S-S) aggregations [systems (d) and (e)] and system (c), precipitation occurs within a short time, but it is required a long time in the (m-E-E) aggregation [systems (a) and (b)]. It is also observed that the precipitation is never observed even after 5 days in the lowest molecular weight PLP sample  $\eta_{Mv} = 7,600$  in W-PrOH (1:9 v/v).

### Observation of Morphology for micro Form I-Aggregates

**The (m-E-E) Aggregation Systems [System (a) and (b) in Table 1].** Figures 1A and 1B show the electron micrographs of Form I of PLP obtained from the (m-E-E) aggregation systems. The samples were prepared in the following way: the systems (a) and (b) in Table 1 are heated up to 65.5 °C, in order to obtain further aggregation. The precipitate was separated from the supernatant liquid and dried for the electron-microscopic examination. In the micrographs, the morphology of Form I shows a rope-type (or fibril-type) aggregate with approximately 10 $\mu$  in diameter ir-



(A)



(B)

**Table 2.** The time ( $t_p$ ) for precipitation of PLP at 65.5 °C

$M_v$	AcOH-PrOH (1:9 v/v)		W-PrOH (1:9 v/v)	
	Form I (after aggre.)	Form I (after aggre.)	Form I (after aggre.)	Form I (after aggre.)
54,000	(a) 52 hr	(c) 5 min	(d) 3 min	(e) 20 min
31,000	(b) 42 hr	(d) 3 min	(e) 20 min	(f) no precipitation
19,000		(e) 20 min	(f) no precipitation	
7,600		(f) no precipitation		

**Figure 1.** An electron micrograph of Form I samples of PLP precipitated from the micro-(E-E) aggregation system (see Table 1); (A): from the system (a) in Table 1; (B): from the system (b).

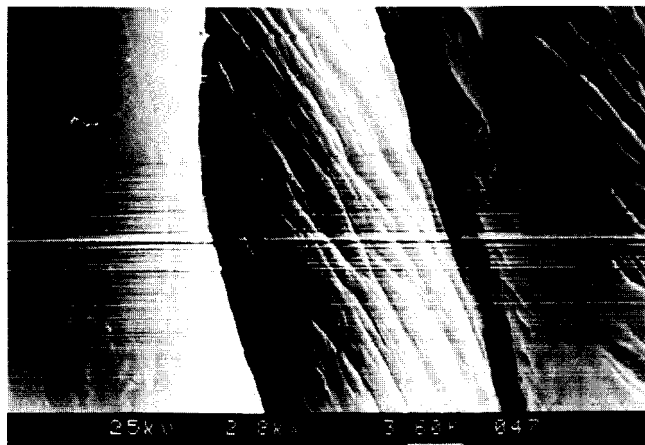
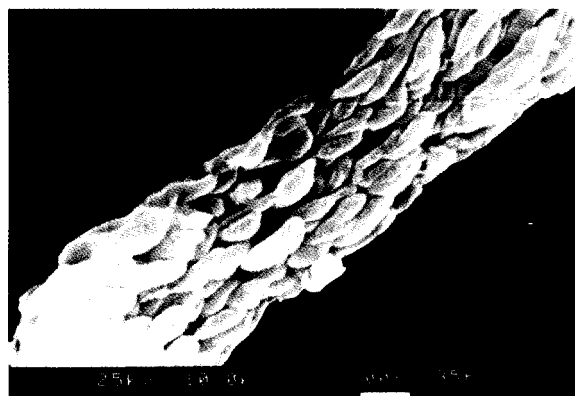


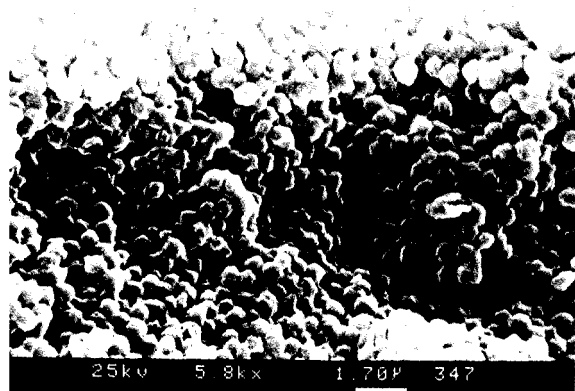
**Figure 2.** A detailed structure of the rope-type aggregate shown in Figure 1B.

respective of molecular weight.

Figure 2 reveals the detail of the rope-aggregate shown in Figure 1B. Although Form I of PLP attains right-handed helix, its compounded precipitate forms a left-handed super helical aggregate, *i.e.*, the super-helix has the opposite sign of molecular conformation. The reason for this phenomenon is not clear at the present, but a similar phenomenon was also observed by other authors<sup>9,10</sup> for poly( $\gamma$ -benzyl-L-glu-



(A)



(B)

**Figure 3.** An electron micrograph of Form I samples of PLP obtained from the micro-(S-S) aggregation system; (A): obtained from the system (d) in Table 1; (B): from the system (e).

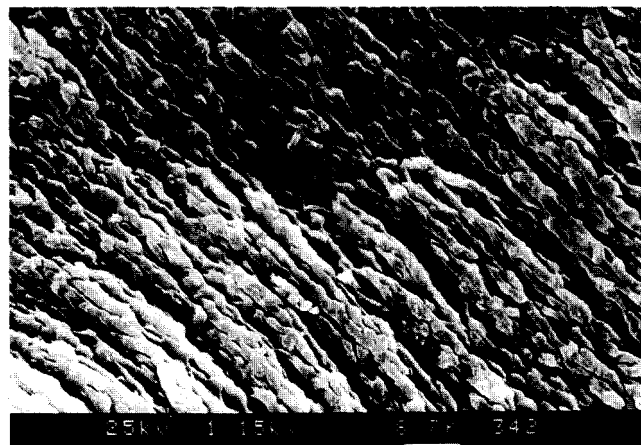


**Figure 4.** An electron micrograph of a Form I sample of PLP obtained from the system (c) in Table 1.

tamate) and poly( $\gamma$ -benzyl-D-glutamate). In Figures 1 and 2, the diameter of the rope is very large 10  $\mu$ . This fact seems to mean that as suggested already by Rybunika and Geil,<sup>9</sup> the thicker ropes appear to be formed by stepwise addition and cooperative twisting of fibrillar strands of various diameter.

**The (m-S-S) Aggregation Systems [System (d) and (e) in Table 1].** For the Form I (m-S-S) aggregation system, we also observed the morphology for the Form I samples precipitated at 65.5  $^{\circ}$ C and the results are shown in Figures 3A and 3B. The morphology of the precipitates shows pebbles type aggregates with a finite size for each pebble in all the systems. The appearance of the pebbles type seems to be due to the following reason: the (m-S-S) aggregation systems attain a saturation at 25  $^{\circ}$ C, but when the temperature was elevated to 65.5  $^{\circ}$ C, further aggregation proceeds by the side-by-side (or raft-like) manner until reaches to a new saturation, which ultimately leads to the precipitation.

In Figure 4 is shown an electron micrograph for the system (c) in Table 1, where an (m-E-E) aggregation occurs following a (m-S-S) aggregation. In this micrograph the form of pebbles is not so clear that the length of the pebbles is not constant. But by a detailed observation, we found that it is a similar pebble type form as in Figure 3. The reason for the unclear pebble type must be due to the coexistence of the (E-E) and (S-S) aggregation.

### The Process of Formation of the Rope- and Pebbles-Type Aggregates

**The Rope-Type Aggregate from the (m-E-E) Aggregate.** In order to investigate how the rope-type aggregates are formed from the (m-E-E) and (m-S-S) aggregates, respectively, we measured the viscosity during the heat-precipitation. Figure 5 shows the curves of  $\eta_{red}$  vs. time at 65.5  $^{\circ}$ C during the precipitation. In the figure the arrow mark indicates the point at which precipitation starts, the time being  $t_p$ . The curves in Figure 5 show a common characteristic: the  $\eta_{red}$  increases at first with time (step 1), after reaching a maximum, it decreases until attains the last value (step 2).

The observation of the rope-type aggregate in Figures 1

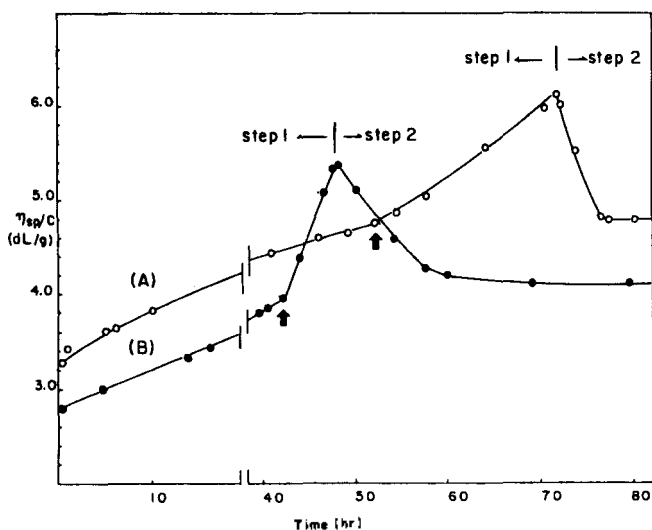


**Figure 5.**  $\eta_{red}$  vs. time during the precipitation occurring at 65.5 °C for the micro-(E-E) aggregation systems; (A): for the system (a) in Table 1; (B): for the system (b).

and 2 and the result of viscosity measurement in Figure 5 lead to propose a reasonable mechanism which is depicted schematically in Figure 6.

In this mechanism, step 1 shows the process of formation of a rope type aggregate with high supercoiling by a quasi-end-to-end manner (*i.e.*, by a partial side-by-side type aggregation which induces a molecule chain length increase<sup>2</sup>). In this step the chain length of PLP is highly increased by this rope-type aggregates, yielding the viscosity increase in Figure 5. In step 2, the rope-type aggregates, which are in a saturated state at the maximum in Figure 5 lead to make entanglement with other rope-type aggregate by a side-by-side manner, this inducing the decrease in viscosity in Figure 5.

**The Pebble-Type Aggregate from the (m-S-S) Aggregate.** In Figure 7 is shown the change of  $\eta_{red}$  vs. time at 65.5 °C for the system of (m-S-S) aggregation during the heat-precipitation. The arrow indicates the time  $t_p$  at which precipitation occurs.

In all the systems except for the system (D),  $\eta_{red}$  decreases monotonically up to the last value, at which occurs a saturation with respect to the aggregation. This result means that the (m-S-S) aggregate which is in a saturation state at room temperature, further side-by-side type (or raft-

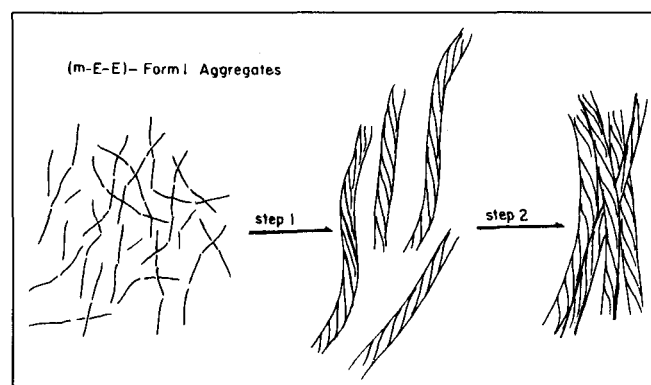


**Figure 6.** Mechanism for the formation of the rope-type aggregates from the micro-(E-E) aggregates.

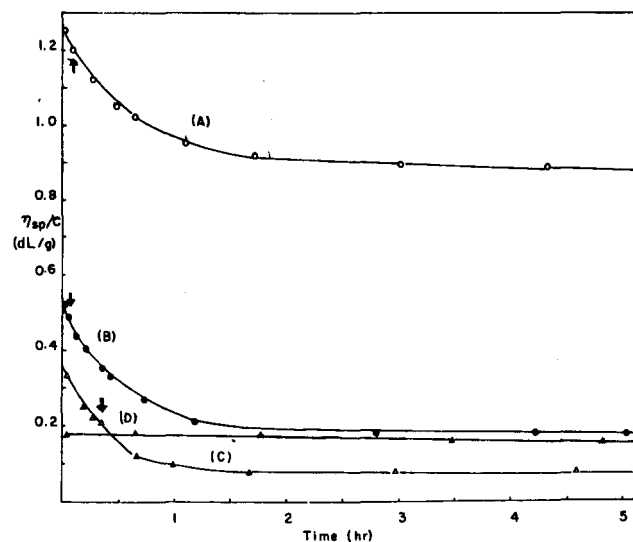


**Figure 7.**  $\eta_{red}$  vs. time during the precipitation at 65.5 °C for the micro-(S-S) aggregation systems; (A): obtained from the system (c), (B): from the system (d), (C): from the system (e), (D): from the system (f).

like) aggregation occurs at 65.5 °C leading to the pebbles-type aggregate with finite pebble size. For curves (A)-(D), explanations are given in the caption. Thus from this result of viscosity measurement we propose the mechanism for the formation of pebbles type aggregate shown in Figure 8.

In the case of the lowest molecular weight PLP sample  $M_w=7,600$  in this study (system (D) in Figure 7), the heat-precipitation does not occur up to even after 5 days. This result is due to the fact as already mentioned in the previous report,<sup>2</sup> an enough Form I units required for the occurrence of (S-S) aggregation are not existed in this sample, thus although the temperature is elevated up to 65.5 °C the (S-S) type aggregation, which ultimately leads to the precipitation, does not occur.

As concluding remarks on the present study from all the results shown in Figures 1 to 8, we know that the morphology of the precipitates depends on the situation in which Form I of PLP was aggregated in the solution prior to the precipitation, *i.e.*, the (m-E-E) and (m-S-S) aggregates of Form I leads to the formation of rope- and pebbles-type aggregation, respectively. Inversely, we find the fact that by the observation and analysis of morphology of precipitates which were produced from the PLP Form I solutions we are able to prove the existence of (m-E-E) and (m-S-S) type aggregates in solution, which already charac-

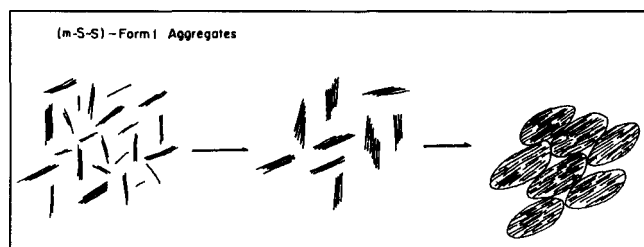


**Figure 8.** Mechanism for the formation of the pebbles-type aggregates from the micro-(S-S) aggregates.

terized by the viscosity and light scattering measurements in the previous reports.

### References

1. Kim, H. D.; Jang, C. H.; Ree, T. J. *Polym. Sci., Polym. Chem. Ed.* **1990**, *28*, 1273.
2. Kim, H. D.; Ree, T. *Bull. Korean. Chem. Soc.* submitted (1997. 2).
3. Wada, A. *Adv. Biophys.* **1976**, *9*, 1-63.
4. Harrington, W. F.; Sela, M. *Biochemica et Biophysica Acta* **1958**, *27*, 24.
5. Ciferri, A.; Orofino, T. A. *J. Phys. Chem.* **1966**, *70*, 3277.
6. Swenson, C. A.; Formanek, R. J. *Phys. Chem.* **1967**, *71*, 4073.
7. Mattice, W. L.; Mandelkern, L. *Macromolecules* **1971**, *4*, 271.
8. Clark, D. S.; Dechter, J. J.; Mandelkern, L. *Biopolymers* **1978**, *17*, 1381.
9. Rybnikar, F.; Geil, P. H. *Biopolymers* **1972**, *11*, 271.
10. Walton, A. G.; Blackwell, J. *Biopolymers*; Academic Press, 1973; p 135-136.

## Interaction of Mastoparan B and Its Ala-Substituted Analogs with Phospholipid Bilayers

Nam Gyu Park, Jung-Kil Seo, Hee-Jung Ku, Seung-Ho Kim\*, Sannamu Lee\*\*, Gohsuke Sugihara\*\*, Kwang-Ho Kim<sup>†</sup>, Jang-Su Park<sup>†</sup>, and Shin-Won Kang<sup>†,\*</sup>

Department of Biotechnology and Bioengineering, College of Fisheries Science, Pukyong National University, Nam-gu, Pusan 608-737, Korea

\*Korea Research Institute of Bioscience and Biotechnology, KIST, Taejeon 305-606, Korea

\*\*Department of Chemistry, Faculty of Science, Fukuoka University, Jonan-ku, Fukuoka 814-01, Japan

<sup>†</sup>Department of Chemistry, College of Natural Science, Pusan National University, Pusan 609-735, Korea

Received February 17, 1997

The interaction of mastoparan B, a tetradecapeptide toxin found in the hornet *Vespa basalis*, with phospholipid bilayers was investigated. Synthetic mastoparan B and its analogs, obtained by substituting one hydrophilic amino acid (2-Lys, 4-Lys, 5-Ser, 8-Ser, 11-Lys, or 12-Lys) in mastoparan B with Ala, were studied. Mastoparan B and its analogs were synthesized by the solid-phase method. As shown by circular dichroism spectra, mastoparan B and its analogs adopted an unordered structure in buffer solution. All peptides took an  $\alpha$ -helical structure, and the  $\alpha$ -helical content of its analogs increased in the presence of neutral and acidic liposomes as compared to that of mastoparan B. In the calcein leakage experiment, we observed that mastoparan B interacted more weakly with lipid bilayers in neutral and acidic media than its analogs. Mastoparan B also showed slightly lower antimicrobial activity and hemolytic activity towards human erythrocytes than its analogs. These results indicate that the greater hydrophobicity of the amphiphilic  $\alpha$ -helix of mastoparan B by replacement with alamine residues results in the increased biological activity and helical content.

### Introduction

Recently, mastoparan B (MP-B), an antimicrobial cationic tetradecapeptide amide, was isolated from the venom of the hornet *Vespa basalis*<sup>1</sup> (Figure 1). MP-B is the mastoparan homolog of vespidae venoms. Mastoparan (MP) has shown various biological activities, such as activation of mast cell degradation histamine release,<sup>2,3</sup> phospholipase A<sub>2</sub><sup>3,4</sup> and C,<sup>4,5</sup> erythrocyte lysis, and binding to calmodulin.<sup>6</sup> In the case of G-protein-coupled receptors *in vitro*,<sup>7</sup> it is obvious that MP enhances the permeability of phospholipid bilayers<sup>8</sup> and activates GTP-binding regulatory proteins (G-proteins). Considering the structure-activity relationship in various natural and synthetic compounds, the amphiphilic  $\alpha$ -helical structure with cationic amino acid residues on one side and hy-

drophobic residues on the other side is closely related to biological activity.<sup>2,9</sup> This structural feature is necessarily important but not itself sufficient to stimulate GTPase of G-protein.<sup>10</sup>

The amino acid sequence of the primary structure of MP-B is very distinct from those of other vespidae mastoparans.<sup>1</sup> Compared to the common structure of vespidae mastoparans (Lys at positions 4, 11 and 12), MP-B has a less hydrophobic sequence at several positions, such as an additional Lys at position 2 and a Trp at position 9. MP-B is a potent stimulator of histamine release from rat peritoneal mast cells, and shows more potent hemolytic activity than MP. MP-B was useful as a cardiovascular depressor<sup>11</sup> and an inhibitor of Gram-positive and -negative bacteria.<sup>12</sup> MP-B showed antimicrobial activity against bacteria and leakage ability.<sup>13</sup> This peptide revealed its amphiphilic properties as shown by helical wheels.<sup>13</sup> MP-B adopts an am-

<sup>\*</sup>Author to whom correspondence should be addressed.